Accepted Manuscript

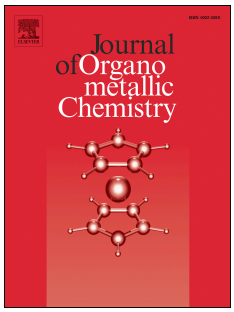

Bis-diorganotin(IV) complexes with binucleating hydraznones derived from a methylene-bis-aromatic aldehyde as linker: Synthesis, spectral and structural characterization, antibacterial activity and DNA cleavage studies

Hamidreza Zafarian, Tahereh Sedaghat, Hossein Motamedi, Damian Trzybiński, Krzysztof Woźniak

PII: S0022-328X(17)30627-7

DOI: 10.1016/j.jorganchem.2017.10.040

Reference: JOM 20160

To appear in: *Journal of Organometallic Chemistry*

Received Date: 31 July 2017

Revised Date: 25 October 2017

Accepted Date: 30 October 2017

Please cite this article as: H. Zafarian, T. Sedaghat, H. Motamedi, D. Trzybiński, K. Woźniak, Bis-diorganotin(IV) complexes with binucleating hydraznones derived from a methylene-bis-aromatic aldehyde as linker: Synthesis, spectral and structural characterization, antibacterial activity and DNA cleavage studies, *Journal of Organometallic Chemistry* (2017), doi: 10.1016/j.jorganchem.2017.10.040.

Bis-diorganotin(IV) complexes with binucleating hydraznones derived from a methylene-bis-aromatic aldehyde as linker: Synthesis, spectral and structural characterization, antibacterial activity and DNA cleavage studies

Hamidreza Zafarian [a], Tahereh Sedaghat [a*], Hossein Motamedi [b,c], Damian Trzybiński[d], Krzysztof Woźniak[d]

[a]*Department of Chemistry, Faculty of Sciences, Shahid Chamran University of Ahvaz, Ahvaz, Iran*

[b]*Department of Biology, Faculty of Sciences, Shahid Chamran University of Ahvaz, Ahvaz, Iran*

[c] *Biotechnology and Biological Science Research Center, Shahid Chamran University of Ahvaz, Ahvaz, Iran*

[d] *Department of Chemistry, Biological and Chemical Research Centre, University of Warsaw, Żwirki i Wigury 101, 02-089 Warszawa, Poland*

**corresponding author: tsedaghat@scu.ac.ir , Fax: 98 611 3331042*

Abstract

Two bis-hydrazone, H_4L^a and H_4L^b, have been synthesized from reaction of 5,5'-methylene-bis-salicylaldehyde with benzhydrazide and furan-2-carbohydrazide, respectively. New organotin(IV) complexes, $(R_2Sn)_2L$ [L = L^a: R = Me (**1**), Ph (**2**); L= L^b: R = Me (**3**), Ph (**4**)] have been synthesized by reaction of dihydrazone ligands with R_2SnCl_2 (R = Me or Ph). The synthesized compounds have been investigated by elemental analysis and IR, ^{1}H NMR, and ^{119}Sn NMR spectroscopy. The structures of **1** and **2** have been also confirmed by X-ray crystallography. The results show that the dihydrazone acts as a tetrabasic ligand in the enolic form and is coordinated to two SnR_2 moieties via ONO donor domains by the imine nitrogen and phenolic and enolic oxygen atoms. All complexes are binuclear and the coordination number of both tin is five. The *in vitro* antibacterial activity of ligands and complexes has been evaluated against Gram-positive (*Bacillus subtilis* and *Staphylococcus aureus*) and Gram-negative (*Escherichia coli* and *Pseudomonas aeruginosa*) bacteria and compared with standard drugs. The synthesized compounds also have been investigated for the chromosomal and plasmid DNA cleavage activity. The complexes significantly inhibited bacterial growth, while none of compounds showed DNA cleavage activity.

Keywords: Hydrazone, Organotin, Antibacterial activity, Binuclear complexes

Introduction

Organotin(IV) chemistry has received continuing attention during the past decades. The considerable interest in these complexes is due to their industrial, agricultural and medicinal applications and the diversity of their structures [1-6]. Among the non-platinum compounds exhibiting anticancer properties, organotin complexes have a valuable place, so that up to now many organotin(IV) compounds have been synthesized and their anticancer activity in comparison to traditional metal anticancer drugs tested [7-10], although the toxicology of organotin compounds may limit their clinical application [11-14]. Biocidal properties of organotin(IV) compounds are dependent on the number and nature of the organic groups, the structure and coordination number of complex and the nature of the donor ligand coordinated to the tin atom [15, 16]. According to the literature, a judicious choice of the ligand attached to the organotin(IV) fragment can improve the biological properties of the complex or reduce side effects [15]. In the field of bioorganotin chemistry one of the interesting research areas is to use bioactive ligands [17]. Among the bioactive ligands, hydrazones are very significant because of their potential biological applications. The study of organotin complexes of hydrazones is highly considered because of their therapeutic and antibacterial activity [18-20].

In the field of hydrazone chemistry, a special place is held by bis-acyl-/aroyl-hydrazones containing amide, azomethine and phenol functional groups. These compounds recently are recognized as polyfunctional ligands and are able to form supramolecular architectures and mono- and polynuclear complexes. A survey of literature shows that although many transition metal complexes of bis-hydrazones have been studied [21], but binuclear organotin(IV) complexes of this type of ligands have not been reported much [22-29]. Bis-acyl-/aroyl-hydrazones can be divided into two basic structural categories: those that are derived from a

dihydrazide and those that are derived from a dialdehyde (or diketone). To our knowledge, despite the some reports about chelating behavior of the former with organotins [22-29], there are no work on structural chemistry of organotin(IV) complexes with the latter.

We have recently reported the synthesis, structural and antibacterial properties of a series of dinuclear organotin(IV) complexes with bis-acyl-hydrazones derived from dihydrazides [24, 25, 27, 29]. In continuation of our research works, in this study we planned to use a methylene-bis-aromatic aldehyde as linkers for the synthesis of two new bis-hydrazones. Then four new dinuclear organotin(IV) complexes have been synthesized from these hydrazones. We visualized that the flexibility or distance introduced in this bifunctional aldehydes may be have advantageous and interesting structural features. Spectral and structural properties and biological activity of ligands and complexes have been reported.

2. Experimental

2.1. Materials and methods

All starting materials were purchased from Merck while diphenyltin dichloride was supplied from Acros Company and all were used as received. Synthesis of 5,5'-methylene-bis-salicylaldehyde involves the use of 1,3,5-trioxane in presence of catalytic amount of conc. H_2SO_4 in glacial CH_3COOH as a solvent according to the procedure described in the literature [30]. The IR spectra were obtained using a FT BOMEM MB102 spectrophotometer. The ^{1}H and ^{119}Sn NMR spectra were recorded with Bruker Avance Ultrashield spectrometers using TMS and $SnMe_4$ as references, respectively. The elemental analyses for C, H, N and S were performed on a Costech-ECS 4010 CHNSO analyzer.

2.2. Synthesis of H_4L^a

5,5'-methylene-bis-salicylaldehyde (0.256 g, 1 mmol) was added to a stirring solution of benzhydrazide (0.272 g, 2 mmol) in ethanol (15 mL). The resulting solution was refluxed for 4 h. The white solid was filtered and washed with ethanol and dried in vacuum over $CaCl_2$. Yield: 0.415 g (84.6%). FT-IR (KBr, cm^{-1}): ν(O–H), 3225; ν(N–H), 3150; ν(Ar–H), 3056; ν(C=O), 1652; ν(C=N), 1619. ^{1}H NMR (250 MHz, DMSO-d_6): δ = 12.05 (s, 2H, OH), 11.03 (s, 2H, NH), 8.60 (s, 2H, CH=N), 7.90 (d, 4H, H1, $^3J_{HH}$ = 6.7 Hz), 7.61-7.48 (m, 6H, $H_{2,3}$), 7.40 (s, 2H, H_a), 7.13 (dd, 2H, H_b, $^3J_{HH}$ = 8.0 Hz), 6.85 (d, 2H, H_c, $^3J_{HH}$ = 8.2 Hz), 3.83 (s, 2H, CH_2).

2.3. Synthesis of H_4L^b

Ligand H_4L^b was synthesized as described for **1** from 5,5'-methylene-bis-salicylaldehyde (0.256 g, 1 mmol) and furan-2-carbohydrazide (0.252 g, 2 mmol) in ethanol (15 mL). The resulting solution was refluxed and the white solid was filtered after 4 h. The product was washed with ethanol and dried in vacuum over $CaCl_2$. Yield: 0.379 g (80.3%). FT-IR (KBr, cm^{-1}): ν(O–H), 3222; ν(N–H), 3150; ν(Ar–H), 3056; ν(C=O), 1658; ν(C=N), 1620. ^{1}H NMR (250 MHz, DMSO-d_6): δ = 12.08 (s, 2H, OH), 10.91 (s, 2H, NH), 8.63 (s, 2H, CH=N), 7.97 (s, 2H, H_1), 7.42 (s, 2H, H_a), 7.31 (d, 2H, H_3, $^3J_{HH}$ = 2.5 Hz), 7.15 (d, 2H, H_b, $^3J_{HH}$ = 7.5 Hz), 6.86 (d, 2H, H_c, $^3J_{HH}$ = 7.5 Hz), 6.72 (s, 2H, H_2), 3.86 (s, 2H, CH_2).

*2.4. Synthesis of $Me_4Sn_2L^a$ (**1**)*

A mixture of H_4L^a (0.123 g, 0.25 mmol) and triethylamine (1 mmol) was stirred in ethanol (10 mL) for 20 min. After this time Me_2SnCl_2 (0.110 g, 0. 5 mmol) in ethanol (5 mL) was added. The solution was refluxed for 4 h. A yellow precipitate was formed during the reaction. The

product was collected, washed with ethanol (5 mL) and dried in vacuum over $CaCl_2$. Yield: 0.141 g (71.9%). Light-yellow plate crystals suitable for X-ray crystallography were obtained in benzene/chloroform solution. Anal. Calcd. for $C_{33}H_{32}N_4O_4Sn_2$: C, 50.4; H, 4.1; N, 7.1%. Found: C, 50.9; H, 3.8; N, 7.4%. FT-IR (KBr, cm^{-1}): ν(C=N), 1616; ν_{as}(Sn–C), 637; ν_s(Sn–C), 570; ν(Sn–O), 527; ν(Sn–N), 451. ^{1}H NMR (250 MHz, DMSO-d_6): δ = 8.81 (s, 2H, CH=N, $^3J(^{119}Sn\text{-}^1H)$ = 43.0 Hz), 8.00 (d, 4H, H_1, $^3J_{HH}$ = 7.3 Hz), 7.53-7.42 (m, 6H, $H_{2,3}$), 7.27 (s, 2H, H_a), 7.16 (d, 2H, H_b, $^3J_{HH}$ = 8.3 Hz), 6.63 (d, 2H, H_c, $^3J_{HH}$ = 8.5 Hz), 3.71 (s, 2H, CH_2), 0.68 [s, 6H, Me_2Sn, $^2J(^{119}Sn\text{-}^1H)$ = 86.8 Hz]. ^{119}Sn NMR (149 MHz, DMSO): δ = –211.3

*2.5. Synthesis of $Ph_4Sn_2L^a$ (**2**)*

Compound **2** was synthesized as described for **1** from H_4L^a (0.123 g, 0.25 mmol), triethylamine (0.5 mmol) and Ph_2SnCl_2 (0.172 g, 0. 5 mmol). Yellow needle crystals suitable for X-ray crystallography were obtained in benzene/chloroform solution.Yield: 0.214 g (82.9%). Anal. Calcd for $C_{53}H_{40}N_4O_4Sn_2$: C, 61.5; H, 3.9; N, 5.4%. Found: C, 61.4; H, 3.6; N, 5.7%. FT-IR (KBr, cm^{-1}): ν(Ar–H), 3053; ν(C=N), 1619; ν(Sn–O), 534; ν(Sn–N), 444. ^{1}H NMR (250 MHz, DMSO-d_6): δ = 8.75 (s, 2H, CH=N, $^3J(^{119}Sn\text{-}^1H)$ = 52.0 Hz), 8.12 (d, 4H, H_1, $^3J_{HH}$ = 7.0 Hz), 7.63 (d, 8H, H_{ortho} of $SnPh_2$, $^3J_{HH}$ = 5.7 Hz), 7.35-7.32 (m, 14H, $H_{meta,para}$ of $SnPh_2$ and H_a), 7.52-7.49 (m, 6H, $H_{2,3}$), 7.22 (d, 2H, H_b, $^3J_{HH}$ = 8.9 Hz), 6.86 (d, 2H, H_c, $^3J_{HH}$ = 8.5 Hz), 3.74 (s, 2H, CH_2). ^{119}Sn NMR (149 MHz, DMSO): δ = –410.7

*2.6. Synthesis of $Me_4Sn_2L^b$ (**3**)*

A mixture of H_4L^b (0.118 g, 0.25 mmol) and triethylamine (1 mmol) was stirred in ethanol (10 mL) for 20 min. Then Me_2SnCl_2 (0.110 g, 0. 5 mmol) in ethanol (5 mL) was added. The solution

was refluxed for 4 h. The product was obtained as yellow solid. The precipitate was filtered, washed with ethanol (5 mL) and dried in vacuum over $CaCl_2$. Yield: 0.588 g (79.2%). Anal. Calcd for $C_{27}H_{28}N_4O_6Sn_2$: C, 43.7; H, 3.8; N, 7.5%. Found: C, 43.4; H, 3.5; N, 7.7%. FT-IR (KBr, cm^{-1}): ν(C=N), 1617; ν_{as}(Sn–C), 625; ν_s(Sn–C), 568; ν(Sn–O), 525; ν(Sn–N), 484. ^{1}H NMR (250 MHz, DMSO-d_6): δ = 8.73 (s, 2H, CH=N, $^3J(^{119}Sn\text{-}^1H)$ = 36.2 Hz), 7.84 (s, 2H, H_1), 7.23 (s, 2H, H_a), 7.14 (d, 2H, H_b, $^3J_{HH}$ = 8.7 Hz), 6.99 (d, 2H, H_3, $^3J_{HH}$ = 3.0 Hz), 6.32-6.60 (m, 4H, $H_{2,c}$), 3.70 (s, 2H, CH_2), 0.67 [s, 6H, Me_2Sn, $^2J(^{119}Sn\text{-}^1H)$ = 88.5 Hz]. ^{119}Sn NMR (149 MHz, DMSO): δ = –224.1

*2.7. Synthesis of $Ph_4Sn_2L^b$ (**4**)*

Compound **4** was synthesized as described for **3** from Ph_2SnCl_2 (0.172 g, 0. 5 mmol). The product was obtained as yellow solid. Yield: 0.214 g (82.9%). Anal. Calcd for $C_{49}H_{36}N_4O_6Sn_2$: C, 58.0; H, 3.6; N, 5.5%. Found: C, 58.2; H, 3.7; N, 5.3%. FT-IR (KBr, cm^{-1}): ν(C=N), 1616; ν(Sn–O), 540; ν(Sn–N), 446. ^{1}H NMR (250 MHz, DMSO-d_6): δ = 8.74 (s, 2H, CH=N, $^3J(^{119}Sn\text{-}^1H)$ = 56.0 Hz), 8.14 (s, 2H, H_1), 8.11 (s, 2H, H_a), 7.64-7.61 (m, 8H, H_{ortho} of $SnPh_2$), 7.57-7.47 (m, 4H, $H_{2,3}$), 7.35-7.33 (m, 14H, $H_{meta,para}$ of $SnPh_2$), 7.20 (d, 2H, H_b, $^3J_{HH}$ = 8.7 Hz), 6.86 (m, 2H, H_c, $^3J_{HH}$ = 8.5 Hz), 3.74 (s, 2H, CH_2). ^{119}Sn NMR (149 MHz, DMSO): δ = –422.0

2.8. Antibacterial tests

In order to evaluate the antibacterial activity of ligand and complexes four different concentrations including 2.5, 5, 10 and 20 mg/mL were prepared in DMSO and sterile blank discs (6.4mm) were saturated by these solutions. So, the effective dose per disc was as 0.1, 0.2, 0.4 and 0.8 mg, respectively. The *Escherichia coli* (ATCC25299), *Pseudomonas aeruginosa*

(ATCC9027), *Bacillus subtilis* (ATCC6633) and *Staphylococcus aureus* (ATCC6538) were selected as target bacterial species and the antibacterial effect of prepared compounds were surveyed according to the Kirby-Bauer standard disc diffusion method. 0.5 McFarland suspensions of bacterial cultures were lawn cultured on Mueller-Hinton agar (MHA, Merck, Germany), the prepared discs were placed on these cultures and plates were incubated at 37°C for 24 h. Finally, the inhibition zone diameter (mm) of each disc was measured and recorded. In order to compare the results, the effect of standard antibiotic discs including Vancomycin, Streptomycin, Penicillin, Nalidixic acid and Gentamicin were studied as previously mentioned. Furthermore, the effect of DMSO saturated disc as negative control was also investigated against bacterial species as previously described.

2.9. Gel electrophoresis assay

The DNA of *B. subtilis* and *E. coli* was extracted by boiling method. One mL of each bacterial suspension was centrifuged at 10000 rpm for 10 min. The precipitate was dissolved in 1 mL of sterile distilled water and boiled for 15 min. The mixture was centrifuged (5000 rpm, 1 min) and the supernatant was harvested and mixed with cold ethanol (2.5 v/v) and stored overnight at -20 °C. Finally, following centrifugation at 13000 rpm for 10 min, the precipitate was dissolved in 100 µL of DNase free sterile water and stored at -20 °C. Plasmid DNA was also extracted by plasmid extraction kit (Qiagen, Germany). 10 µL of 20 mg/mL solution of each compound in DMSO was mixed with 10 µL of DNA and incubated at 37 °C for 2 h. A positive control was also prepared by mixing 10 µL of H_2O_2 with 10 µL of DNA and untreated DNA was regarded as negative control. These DNA samples were electrophoresed in 1% agarose containing DNA safe

stain at 100 V for 50 min. A 1 Kb DNA ladder was used as size marker. The gel was documented with UVI-Tec gel documentation system.

2.10. X-ray structure determination

Good quality single-crystals of **1** and **2** were selected for the X-ray diffraction experiments. Diffraction data were collected at T = 100(2) K on the Agilent Technologies SuperNova Dual Source (**1**) and Agilent Technologies Supernova Single Source (Mo) (**2**) diffractometers with Mo$K\alpha$ radiation (λ = 1.54184 Å) using CrysAlis RED software [31]. In both cases the analytical numerical absorption correction using a multifaceted crystal model based on expressions derived by R.C. Clark & J.S. Reid [32] implemented in SCALE3 ABSPACK scaling algorithm, was applied [31]. The structural determination procedure was carried out using the SHELX package [33]. The structures were solved with direct methods and then successive least-square refinement was carried out based on the full-matrix least-squares method on F^2 using the XLMP program [33]. All H-atoms were positioned geometrically, with the C–H bond lengths set to be equal to 0.93 and 0.96 Å for the aromatic and methyl H-atoms, respectively, and constrained to ride on their parent atoms with $U_{iso}(H) = xU_{eq}(C)$, where x = 1.2 for the aromatic, and x = 1.5 for the methyl H-atoms. In the case of **2**, few distinct peaks on the difference Fourier map are indicating the presence of a disordered solvent molecule. All attempts to model this small disorder of solvent molecules used for crystallization failed. Therefore, the solvent contribution has been removed applying the appropriate MASK procedure in the Olex2 program [34]. Calculated void volume was approximately 491.7 $Å^3$ occupied by 49.6 electrons per unit cell. The figures for this publication were prepared using Olex2 and ORTEP-3 programs [34, 35]. The molecular interactions in crystals were identified using PLATON [36].

3. Results and discussion

Dihydrazones, H_4L^a and H_4L^b, have been obtained from condensation of 5,5'-methylene-bis-salicylaldehyde with benzhydrazide and furan-2-carbohydrazide, respectively. Therefore methylene-bis-aromatic aldehyde acts as flexible linker for the preparation of binucleating ligands (Figure 1). The flexibility present in the $–CH_2–$ moiety of the linker allows the ligand or their complexes to adopt different orientations. It may be supposed that in solution there is a fast dynamic equilibrium between different conformations [37]. These bis-hydrazone ligands have potentially six donor atoms with four ionizable protons and two tridentate domain.

The binuclear organotin complexes **1**-**4** (Figure 1) were prepared by reaction of H_4L^a and H_4L^b with R_2SnCl_2 (R = Me and Ph) in presence of triethylamine in 1:2:4 ratio. The new complexes were characterized by elemental analysis and IR, ^1H and ^{119}SnNMR spectroscopy. Stoichiometry of the complexes was confirmed by analytical data and the integrated ^1H NMR spectra. The structure of **1**and **2** has been also determined by X-ray diffraction.

3.1. X-ray structures

The identity of **1** and **2** was proven by the single-crystal X-ray diffraction analysis. It turned out that the complex **1** crystallizes in the monoclinic $P2_1/c$ space group with four molecules of compound in the unit cell (one in the asymmetric part of the unit cell), whereas the compound **2** is crystallizes in triclinic *P*-1 space group and in this case two molecules of complex are present in the unit cell (again one in the asymmetric part of the unit cell - see Figure 2). The details of crystallographic data and the refinement parameters are summarized in Table 1. Selected bond lengths and angles are listed in Tables 2 and 3. Both investigated complexes are binuclear and structural parameters describing two parts of molecule are similar. The dihydrazone moiety acts

as a tetrabasic ligand and exists in the enol form. It is coordinated to the two Sn atoms *via* the imine nitrogen atom and the enolate, and phenolate oxygen atoms. Thus each tridentate pocket forms six and five-membered chelate ring around the SnR_2 moiety. Above-mentioned chelate rings are not planar, however the values of the torsion angles describing these molecular fragments are quite small (Tables 2 and 3). The coordination sphere of each Sn atom is completed by two carbon atoms of organic groups. Therefore, the coordination number of each Sn atoms is five. The index of trigonality, τ, can be defined: $\tau = (\alpha - \beta)/60$, and it quantifies the extent of distortion from either the ideal square pyramid or trigonal bipyramid, wherein α and β are the two largest bond angles around the metal atom in the five-coordinated environment [38]. The trigonality index is equal to zero for an ideal square pyramidal geometry, while it becomes unity for ideal trigonal bipyramidal geometry. In the complex **1,** the τ value is 0.335 and 0.411 for Sn1 and Sn2 atoms, respectively, therefore the metal coordination geometry around both Sn atoms can be described as highly distorted square pyramid. This distortion from perfect geometries is mainly due to the rigidity of chelate rings, and facilitated by the large covalent radius of tin(IV) [39, 40]. The imine nitrogen is chosen as apex of square pyramid because any four donor atoms which define the two largest angles, α and β, should not be in apical position. According to the complex **2** in this case the trigonality index is 0.427 and 0.520 for Sn1 and Sn2 atoms, respectively. These values indicate that the geometry around the Sn1 atom is highly distorted square pyramid with one of the phenyl carbon atoms occupying the axial position. The Sn2 atom coordination geometry is almost midway the idealized square-pyramidal and trigonal-bipyramidal geometries. However, with particular precision, trigonal-bipyramidal with oxygen atoms in the axial positions predominates. As in the case of **1,** distortions from the ideal

geometries in **2** are mainly caused by the rigidity of chelate rings, and facilitated by the large covalent radius of tin (IV).

The Sn−N bond lengths are very similar to the sum of the covalent radii of Sn−N (2.15 Å), but are considerably shorter than the sum of Van der Waals radii (3.75 Å) [41, 42]. The $Sn-O_{phenolic}$ and $Sn-O_{enolic}$ distances are also similar to the sum of the covalent radii of Sn−O (2.10 Å). Therefore, there is a very strong covalent bond between tin and oxygen and nitrogen atoms. In the complex **1,** the difference between the C−Sn−C angle from the X-ray diffraction data, 134.85° and 130.13°, and the empirical estimation in solution (139.4° and 141.9°) calculating in section 3.2, may be related to the removal of the crystal network pressure in solution and also probable interaction with DMSO as a coordinating solvent.

In the crystal of **1**, adjacent molecules of the investigated complex are held together by the weak C−H···N hydrogen bonds and C−H···π contacts (Tables 1S and 2S) and this results in the formation of infinite chains running along crystallographic b-direction (Figure 3a). Neighboring chains in the crystal structure are further stabilized by the network of C−H···π intermolecular interactions (Table 2S) and, finally, a complex supramolecular framework arises (Figure 3b).

In the case of **2,** the adjacent molecules of the complex are involved in the network of intermolecular C−H···π contacts (Figure 4, Table 3S). These weak interactions stabilize the crystal structure.

3.2. Spectroscopic studies

In the IR spectra of free ligands a band observed about 3220 cm^{-1} is attributable to stretching vibration of OH indicating inter-/intra-molecular hydrogen bonding. In the spectra of complexes

the absence of any bands for ν(O-H), ν(N-H) and ν(C=O) shows the complete deprotonation of the ligand and coordination with tin in the enolate form [18]. The ν(C=N) band which appears about 1620 cm^{-1} in the spectra of ligands is shifted to a lower frequency for complexes. This observation indicates that the imine nitrogen atom is involved in coordination to the tin. In the IR spectra of complexes new bands were observed in the range ~400-600 cm^{-1} related to Sn–N and Sn–O stretching frequency. The appearance of these bands confirms coordination of nitrogen and oxygen to the tin atom [43-45]. Presence of both ν_s(Sn–C) and ν_{as}(Sn–C) in the IR spectrum of **1** and **3** suggests a nonlinear Me-Sn-Me configuration.

The ^{1}H NMR spectral data of complexes in DMSO is presented in the experimental section according to the atomic numbering shown in Figure 1. The complete absence of the signals due to the acidic protons, –NH-N= and Ar-OH, suggests the complete deprotonation of ligand and coordination to the tin in the enolate form. In the ^{1}H NMR spectra of complexes, the ratio of the integrals of the signals from the protons of the ligand to the protons of the organic groups on the tin confirms a 2:1 ratio of metal to ligand in the complexes. The appearance of only one set of signals in ^{1}H NMR of H_2L^a and H_2L^b shows the magnetically equivalence of two the parts of molecules. A signal attributed to two imine protons in the spectrum of free ligands is slightly shifted downfield and accompanied by satellites due to $^3J(^{119}Sn\text{-}H)$ coupling in all complexes. Appearance of only one signal for both imine protons flanked by satellites is an evidence that the two imine nitrogen atoms are magnetically equivalent in solution and both are coordinated to tin(IV) centers. The ^{1}HNMR spectrum of **1** and **3** shows a singlet at upfield for $SnMe_2$ protons accompanied by satellites due to $^2J(^{119}Sn\text{-}^1H)$. This coupling constant is larger than uncomplexed Me_2SnCl_2 (68.7 Hz) indicates the increasing coordination number of tin [26].

Substitution of $^{2}J(^{119}Sn\text{-}^{1}H)$ in the Lockhart-Manders equation [46], $\theta = 0.016|^{2}J|^{2} - 1.32|^{2}J| + 133.4$, gives a value of 139.4° and 141.9° for Me-Sn-Me angles in **1** and **3**, respectively.

The ^{119}Sn NMR spectra of all complexes show only one sharp singlet indicates the existence of a single species in solution and show the similar environment for both tin centers in complex. The ^{119}Sn chemical shifts show large up-field shift in comparison to the original Me_2SnCl_2 (+137 ppm) and Ph_2SnCl_2 (-32 ppm) [47] which is in agreement with the increasing of the coordination number of tin. These shifts are in the range reported empirically for five-coordinate diorganotin(IV) complexes [37, 48-50], therefore the coordination number of both tin in binuclear complexes is five in solution. The chemical shifts are appeared at up-field for diphenyltin complexes in comparison to dimethyl ones, due to anisotropic shielding effects and pi interactions [26].

3.3. Antibacterial activity and DNA cleavage

The synthesized ligands and their organotin(IV) complexes were screened against *Bacillus subtilis* and *Staphylococcus aureus* (as Gram-positive bacteria) and *Escherichia coli* and *Pseudomonas aeruginosa* (as Gram-negative bacteria) to assess their antibacterial activity. The results are given in Table 4 in comparison with the standard antibacterial drugs, *viz*, Vancomycin, Streptomycin, penicillin, Nalidixic acid and Gentamycin. An inhibition zone diameter over 7 mm can represent activity against bacteria under investigation [51] . The synthesized compounds also have been investigated for their chromosomal and plasmid DNA cleavage activity by agarose gel electrophoresis method.

The results showed the free ligands are inactive against all tested bacteria. While all complexes, except **4** against *E.coli*, significantly inhibited bacterial growth. None of compounds

showed DNA cleavage activity against both chromosomal and plasmid DNA. The enhanced antibacterial activity of the ligand on complexation with organotin(IV) precursors can be explained according to Overton's concept and Tweedy's chelation theory [52, 53], as well as it may be due to the intrinsic biological activity effects of organotin moiety [15, 27, 54]. On the basis of Overton's concept, lipophilicity is an important factor, which controls the antimicrobial activity, because the lipid layer of the cell membrane favors the permeation of only the lipid-soluble materials, i.e., hydrophobic substances. According to chelation theory, the polarity of metal ions will be reduced upon complexation. As consequence, upon complexation the lipophilic nature of the central Sn atom enhances which favors the passage of the complexes through cell membrane [24, 29, 55-60]. Two main factors are responsible for this reduction in polarity; firstly the partial sharing of metal positive charge with donor atoms of ligand and secondly the overlap of ligand orbitals and electron delocalization over the whole chelate [61]. The higher activity of **1** and **2** than **3** and **4** may also be attributed to the lipophilicity increased by the presence of two phenyl groups instead of furan rings. It is noteworthy that all complexes especially **1** are remarkably active against *P. aeruginosa* while, the bacteria of the genus *Pseudomonas* are resistant to many standard drugs [62, 63].

According to the results of antibacterial activity and DNA cleavage, all complexes can inhibit the growth and multiplication of the bacteria by affecting bacterial cell envelope or possibly interfering with metabolic pathways whereas, it is not harmful for DNA structure. The absence of destructive effect on bacterial DNA can be an advantage; hence these complexes can be used safely for bacterial growth control in environment without any side effects on eukaryotic DNA. In other word, these compounds will not be mutagen for eukaryotic cells.

Comparing the results of this research with our previous works [24, 27, 29, 54, 55, 60, 64] confirm that the lipophilicilty of both organic groups and donor ligand coordinated to the organotin(IV) fragment has a great impact on the improvement of biological properties of organotin(IV) compounds. Therefore a judicious choice of organic groups and the substituents in the donor ligand can modulate the activity of the complex. Among the studied diorganotin(IV) complexes, the high activity was exerted by $[Ph_2Sn(IV)]^{2+}$ complexes.

Conclusion

Dihydrazones which contain two similar ONO tridentate domains, are completely deprotonated and bonded to two diorganotin moiety via the imine nitrogen and phenolic and enolic oxygen atoms. All complexes are binuclear and both tin atoms have similar environment with coordination number of five. In most cases, the complexes exhibit significantly antibacterial activity against all tested bacteria, but do not show any DNA cleavage activity. Therefore DNA cleavage is not considered as a bactericidal mechanism for these complexes.

Acknowledgment

Support of this work by Shahid Chamran University of Ahvaz, Ahvaz, Iran (Grant No. 1396) is gratefully acknowledged. The crystallographic part of this study was carried out at the Biological and Chemical Research Centre, University of Warsaw, established within the project co-financed by European Union from the European Regional Development Fund under the Operational Programme Innovative Economy, 2007 – 2013. This study was also supported by the National Science Centre Poland MAESTRO grant-DEC-2012/04/A/ST5/00609 (DT and KW), which enabled the X-ray structural analysis to be performed.

Appendix A. Supplementary material

CCDC 1517341 and 1517372 contains the supplementary crystallographic data for **1** and **2**, respectively. These data can be obtained free of charge via http://www.ccdc.cam.ac.uk/conts/retrieving.html, or from the Cambridge Crystallographic Data Centre, 12 Union Road, Cambridge CB2 1EZ, UK; fax: +44 1223 336 033; or e-mail: deposit@ccdc.cam.ac.uk.

References

[1] P.J. Smith, Chemistry of tin, Springer Science & Business Media, 2012.

[2] M. Gielen, Tin chemistry: fundamentals, frontiers, and applications, John Wiley & Sons, 2008.

[3] S. Etezadi, A. Koppaka, M.M. Gamage, B. Captain, J. Organomet. Chem., 848 (2017) 122-132.

[4] A. Koppaka, L. Zhu, V. Yempally, D. Isrow, P.J. Pellechia, B. Captain, J. Am. Chem. Soc., 137 (2014) 445-456.

[5] O.T. Summerscales, M.M. Olmstead, P.P. Power, Organometallics, 30 (2011) 3468-3471.

[6] K.K. Pandey, P.P. Power, Organometallics, 30 (2011) 3353-3361.

[7] M.K. Amir, S. Khan, R. Zia ur, A. Shah, I.S. Butler, Inorg. Chim. Acta, 423 (2014) 14-25.

[8] C.E. Carraher, M.R. Roner, J. Organomet. Chem., 751 (2014) 67-82.

[9] S.K. Hadjikakou, N. Hadjiliadis, Coord. Chem. Rev., 253 (2009) 235-249.

[10] F. Arjmand, S. Parveen, S. Tabassum, C. Pettinari, Inorg. Chim. Acta, 423 (2014) 26-37.

[11] T. Hamasaki, T. Sato, H. Nagase, H. Kito, Mutat. Res. Gen. Toxicol., 300 (1993) 265-271.

[12] J.S. White, J.M. Tobin, J.J. Cooney, Can. J. Microbiol., 45 (1999) 541-554.

[13] L. Niu, Y. Li, Q. Li, Inorg. Chim. Acta, 423 (2014) 2-13.

[14] A. Pagliarani, S. Nesci, V. Ventrella, Toxicol. in Vitro, 27 (2013) 978-990.

[15] C. Pellerito, L. Nagy, L. Pellerito, A. Szorcsik, J. Organomet. Chem., 691 (2006) 1733-1747.

[16] X. Song, A. Zapata, G. Eng, J. Organomet. Chem., 691 (2006) 1756-1760.

[17] L. Pellerito, L. Nagy, Coord. Chem. Rev., 224 (2002) 111-150.

[18] K. Liu, H. Yan, G. Chang, Z. Li, M. Niu, M. Hong, Inorg. Chim. Acta, 464 (2017) 137-146.

[19] Y. Yang, M. Hong, L. Xu, J. Cui, G. Chang, D. Li, C.-z. Li, J. Organomet. Chem., 804 (2016) 48-58.

[20] C. González-García, A. Mata, F. Zani, M.A. Mendiola, E. López-Torres, J. Inorg. Biochem., 163 (2016) 118-130.

[21] A.-M. Stadler, J. Harrowfield, Inorg. Chim. Acta, 362 (2009) 4298-4314.

[22] M.P. Degaonkar, V.G. Puranik, S.S. Tavale, S. Gopinathan, C. Gopinathan, B. Chem. Soc. Jpn, 67 (1994) 1797-1801.

[23] H.-d. Yin, J.-c. Cui, Y.-l. Qiao, Polyhedron, 27 (2008) 2157-2166.

[24] T. Sedaghat, M. Aminian, G. Bruno, H. Amiri Rudbari, J. Organomet. Chem., 737 (2013) 26-31.

[25] T. Sedaghat, M. Aminian, H. Amiri Rudbari, G. Bruno, J. Organomet. Chem., 754 (2014) 26-31.

[26] S. Shujah, N. Muhammad, A. Shah, S. Ali, A. Meetsma, Z. Hussain, J. Organomet. Chem., 759 (2014) 19-26.

[27] T. Sedaghat, M. Aminian, M. Azarkish, Phosphorus, Sulfur, and Silicon and the Related Elements, 190 (2015) 352-359.

[28] D.K. Dey, S.P. Dey, N.K. Karan, A. Lyčka, G.M. Rosair, J. Organomet. Chem., 749 (2014) 320-326.

[29] H. Zafarian, T. Sedaghat, H. Motamedi, H.A. Rudbari, J. Organomet. Chem., 825 (2016) 25-32.

[30] C. Marvel, N. Tarköy, J. Am. Chem. Soc., 79 (1957) 6000-6002.

[31] CrysAlis CCD and CrysAlis Red, Oxford Diffraction, Oxford Diffraction Ltd, Yarnton, England, 2008.

[32] R. Clark, J. Reid, Acta Cryst. Sect. A 51 (1995) 887-897.

[33] G.M. Sheldrick, Acta Crystallogr., Sect. A: Found. Crystallogr., 64 (2008) 112-122.

[34] O.V. Dolomanov, L.J. Bourhis, R.J. Gildea, J.A. Howard, H. Puschmann, J. Applied Cryst., 42 (2009) 339-341.

[35] L.J. Farrugia, J. Appl. Cryst., 45 (2012) 849-854.

[36] A. Spek, Acta Cryst. D, 65 (2009) 148-155.

[37] V. Barba, E. Vega, R. Luna, H. Höpfl, H.I. Beltrán, L.S. Zamudio-Rivera, J. Organomet. Chem., 692 (2007) 731-739.

[38] A.W. Addison, T.N. Rao, J. Reedijk, J. van Rijn, G.C. Verschoor, J. Chem. Soc., Dalton Trans., (1984) 1349-1356.

[39] C. Pettinari, F. Marchetti, R. Pettinari, D. Martini, A. Drozdov, S. Troyanov, Inorg. Chim. Acta, 325 (2001) 103-114.

[40] S. Öztaş, E. Şahin, N. Ancın, S. Ide, M. Tüzün, J. Mol. Struct., 705 (2004) 107-112.

[41] B. Cordero, V. Gómez, A.E. Platero-Prats, M. Revés, J. Echeverría, E. Cremades, F. Barragán, S. Alvarez, Dalton Trans., (2008) 2832-2838.

[42] S. Batsanov, Inorg. materials, 37 (2001) 871-885.

[43] T. Sedaghat, M. Naseh, G. Bruno, H.A. Rudbari, H. Motamedi, J. Coord. Chem., 65 (2012) 1712-1723.

[44] B. Yearwood, S. Parkin, D.A. Atwood, Inorg. chim. Acta, 333 (2002) 124-131.

[45] D.K. Dey, S.P. Dey, N.K. Karan, A. Datta, A. Lycka, G.M. Rosair, J. Organomet. Chem., 694 (2009) 2434-2441.

[46] T.P. Lockhart, W.F. Manders, Inorg. Chem., 25 (1986) 892-895.

[47] R. Palchaudhuri, P.J. Hergenrother, Curr. Opin. Biotech., 18 (2007) 497-503.

[48] J. Otera, Journal of Organometallic Chemistry, 221 (1981) 57-61.

[49] D. Kovala-Demertzi, P. Tauridou, U. Russo, M. Gielen, Inorg. Chim. Acta, 239 (1995) 177-183.

[50] J. Otera, A. Kusaba, T. Hinoishi, Y. Kawasaki, J. Organomet. Chem., 228 (1982) 223-228.

[51] M.S. Refat, I.M. El-Deen, Z.M. Anwer, S. El-Ghol, J. Mol. Struct., 920 (2009) 149-162.

[52] B. Tweedy, Phytopathology, 55 (1964) 910-914.

[53] Y. Anjaneyulu, R.P. Rao, Synth.React.Inorg.Met.-Org. Chem., 16 (1986) 257-272.

[54] T. Sedaghat, L. Tahmasbi, H. Motamedi, R. Reyes-Martinez, D. Morales-Morales, J. Coord. Chem., 66 (2013) 712-724.

[55] M. Khandani, T. Sedaghat, N. Erfani, M.R. Haghshenas, H.R. Khavasi, J. Mol. Struct., 1037 (2013) 136-143.

[56] R.V. Singh, P. Chaudhary, S. Chauhan, M. Swami, Spectrochim. Acta, Part A, 72 (2009) 260-268.

[57] B. Ruan, Y. Tian, R. Hu, H. Zhou, J. Wu, J. Yang, H. Zhu, Inorg. Chim. Acta, 365 (2011) 473-479.

[58] M. Affan, M. Salam, F.B. Ahmad, F. White, H.M. Ali, Inorg. Chim. Acta, 387 (2012) 219-225.

[59] F. Shaheen, S. Ali, A. Meetsma, Polyhedron, 31 (2012) 697-703.

[60] T. Sedaghat, Y. Ebrahimi, L. Carlucci, D.M. Proserpio, V. Nobakht, H. Motamedi, M.R. Dayer, J. Organomet. Chem., 794 (2015) 223-230.

[61] S. Shujah, N. Muhammad, S. Ali, N. Khalid, M.N. Tahir, J. Organomet. Chem., 696 (2011) 2772-2781.

[62] R. Juan-Luis, F. Alian, Pseudomonas, Virulence and gene regulation, Springer, 2007.

[63] D.M. Livermore, Clin. Infect. Dis., 34 (2002) 634-640.

[64] T. Sedaghat, M. Yousefi, G. Bruno, H. Amiri Rudbari, H. Motamedi, V. Nobakht, Polyhedron, 79 (2014) 88-96.

Table 1 Crystallographic and structure refinement data for **1** and **2**

Identification code	**1**	**2**
Empirical formula	$C_{33}H_{32}N_4O_4Sn_2$	$C_{53}H_{40}N_4O_4Sn_2$
Formula weight	786.01	1034.27
Temperature/K	100(2)	100(2)
Crystal system	monoclinic	triclinic
Space group	$P2_1/c$	P-1
a/Å	8.5659(3)	9.61550(12)
b/Å	25.8115(8)	14.91495(19)
c/Å	14.1311(4)	18.6982(2)
α/°	90.00	104.6543(11)
β/°	96.235(3)	91.3668(10)
γ/°	90.00	101.6051(10)
Volume/Å^3	3105.88(17)	2533.41(5)
Z	4	2
ρ_{calc}g/cm^3	1.681	1.356
μ/mm^{-1}	1.652	1.031
F(000)	1560.0	1036.0
Crystal size/mm	0.28 × 0.22 × 0.06	0.52 × 0.09 × 0.07
Radiation	Mo$K\alpha$ (λ = 0.71073)	Mo$K\alpha$ (λ = 0.71073)
2Θ range for data collection/°	3.3 to 56.56	3.16 to 52.74
Index ranges	$-11 \le h \le 11$, $-34 \le k \le 34$, $-18 \le l \le 18$	$-14 \le h \le 14$, $-22 \le k \le 22$, $-28 \le l \le 28$
Reflections collected	39128	162028
Independent reflections	7718 [R_{int} = 0.0380, R_{sigma} = 0.0293]	10337 [R_{int} = 0.0403, R_{sigma} = 0.0212]
Data/restraints/parameters	7718/0/392	10337/0/568
Goodness-of-fit on F^2	1.063	1.070
Final R indexes [I>=2σ (I)]	R_1 = 0.0329, wR_2 = 0.0726	R_1 = 0.0271, wR_2 = 0.0724
Final R indexes [all data]	R_1 = 0.0426, wR_2 = 0.0781	R_1 = 0.0302, wR_2 = 0.0747
Largest diff. peak/hole / e Å^{-3}	1.39/-0.64	1.25/-0.43

Table 2. Bond lengths [Å] and angles [°] for complex **1**

Sn1–O1	2.151(2)	C1–O1	1.297(4)
Sn1–O2	2.092(2)	C1–N1	1.308(4)
Sn1–C15	2.110(3)	N1–N2	1.395(3)
Sn1–C16	2.108(4)	N2–C2	1.302(4)
Sn1–N2	2.185(2)	C4–O2	1.316(4)
Sn2–O3	2.149(2)	C18–O3	1.302(4)
Sn2–O4	2.085(2)	C18–N3	1.308(4)
Sn2-C32	2.117(3)	N3–N4	1.396(3)
Sn2–C33	2.095(3)	N4–C19	1.305(4)
Sn2–N4	2.186(3)	C21–O4	1.324(4)
O1–Sn1-O2	154.97(9)	O3–Sn2–O4	154.85(8)
O1–Sn1–C15	93.78(11)	O3–Sn2–C32	94.67(11)
O1–Sn1–C16	92.18(12)	O3–Sn2–C33	95.65(12)
O2–Sn1–C15	91.59(12)	O4–Sn2–C32	97.53(12)
O2–Sn1–C16	101.22(13)	O4–Sn2–C33	93.16(12)
O1–Sn1–N2	72.87(9)	O3–Sn2–N4	72.31(9)
C15–Sn1–C16	134.84(13)	C32–Sn2–C33	130.14(13)
O2–Sn1–N2	82.98(9)	O4–Sn2–N4	82.55(9)
N2–Sn1–C15	117.66(11)	N4–Sn2–C32	117.04(12)
N2–Sn1–C16	106.87(11)	N4–Sn2–C33	112.58(12)
N1– C1–O1–Sn1	-2.0(4)	N3 –C18–O3–Sn2	-13.5(4)
C3–C4–O2–Sn1	10.9(5)	C20–C21–O4–Sn2	-26.9(4)
C3–C2–N2 –Sn1	-4.2(5)	C20–C19–N4–Sn2	-0.7(5)
C1–N1–N2–Sn1	2.8(3)	C18–N3–N4–Sn2	9.9(3)

Table 3. Bond lengths [A] and angles [°] for complex **2**

Sn1-O1	2.1192(16)	C1–O1	1.302(3)
Sn1-O2	2.0691(15)	C1–N1	1.309(3)
Sn1-C15	2.114(2)	N1–N2	1.399(2)
Sn1-C21	2.114(2)	N2–C2	1.296(3)
Sn1-N2	2.1673(18)	C4–O2	1.332(3)
Sn2-O3	2.1144(17)	C28–O3	1.299(3
Sn2-O4	2.1144(17)	C28–N3	1.304(3)
Sn2-C48	2.118(2)	N3–N4	1.399(3)
Sn2-C42	2.112(3)	N4–C29	1.296(3)
Sn2-N4	2.1594(19)	C31–O4	1.319(3)
O1-Sn1-O2	154.89(6)	O3-Sn2-O4	157.17(7)
O1-Sn1-C15	93.30(8)	O3-Sn2-C42	96.24(10)
O1-Sn1-C21	105.54(8)	O3-Sn2-C48	94.58(9)
O2-Sn1-C15	92.40(8)	O4-Sn2-C42	96.62(10)
O2-Sn1-C21	100.51(8)	O4-Sn2-C48	94.17(9)
O1-Sn1-N2	73.16(6)	O3-Sn2-N4	73.40(7)
C15-Sn1-C21	124.75(8)	C42-Sn2-C48	122.85(9)
O2-Sn1-N2	84.34(6)	O4-Sn2-N4	84.41(7)
N2-Sn1-C15	129.22(7)	N4-Sn2-C42	110.94(9)
N2-Sn1-C21	105.54(8)	N4-Sn2-C48	125.92(8)
N1– C1–O1–Sn1	-8.2(3)	N3 –C28–O3–Sn2	7.3(3)
C3–C4–O2–Sn1	17.6(3)	C30–C31–O4–Sn2	12.7(3)
C3–C2–N2 –Sn1	-8.3(3)	C30–C29–N4–Sn2	1.1(3)
C1–N1–N2–Sn1	4.3(2)	C28–N3–N4–Sn2	9.9(3)

Table 4 Antibacterial activity data of ligands and organotin(IV) complexes

Compound	Conc. (mg/disc)	Inhibition zone (mm)			
		E. Coli	*P. aeruginosa*	*S. aureus*	*B. subtilis*
H_4L^a	0.1	n.a.	n.a.	n.a.	n.a.
	0.2	n.a.	n.a.	n.a.	n.a.
	0.4	n.a.	n.a.	n.a.	n.a.
	0.8	n.a.	n.a.	n.a.	n.a.
H_4L^b	0.1	n.a.	n.a.	n.a.	n.a.
	0.2	n.a.	n.a.	n.a.	n.a.
	0.4	n.a.	n.a.	n.a.	n.a.
	0.8	n.a.	n.a.	n.a.	n.a.
$Sn_2Me_2L^a$ (**1**)	0.1	20	19	19	20
	0.2	21	19	19	20
	0.4	21	20	19	20
	0.8	23	21	22	21
$SnPh_4L^a$ (**2**)	0.1	11	21	17	10
	0.2	11	22	17	13
	0.4	12	22	18	13
	0.8	14	25	25	19
$SnMe_2L^b$ (**3**)	0.1	n.a.	9	13	n.a.
	0.2	11	9	14	8
	0.4	11	11	16	9
	0.8	15	11	17	12
$SnPh_4L^b$ (**4**)	0.1	n.a.	15	15	12
	0.2	n.a.	16	16	12
	0.4	n.a.	20	18	13
	0.8	n.a.	21	19	16
Vancomycin	30	14	n.a.	17	24
Streptomycin	10	16	n.a.	12	22
Penicilin	10	12	n.a.	26	13
Nalidixic acid	30	25	n.a.	12	23
Gentamicin	10	20	20	16	21

n.a. = no activity

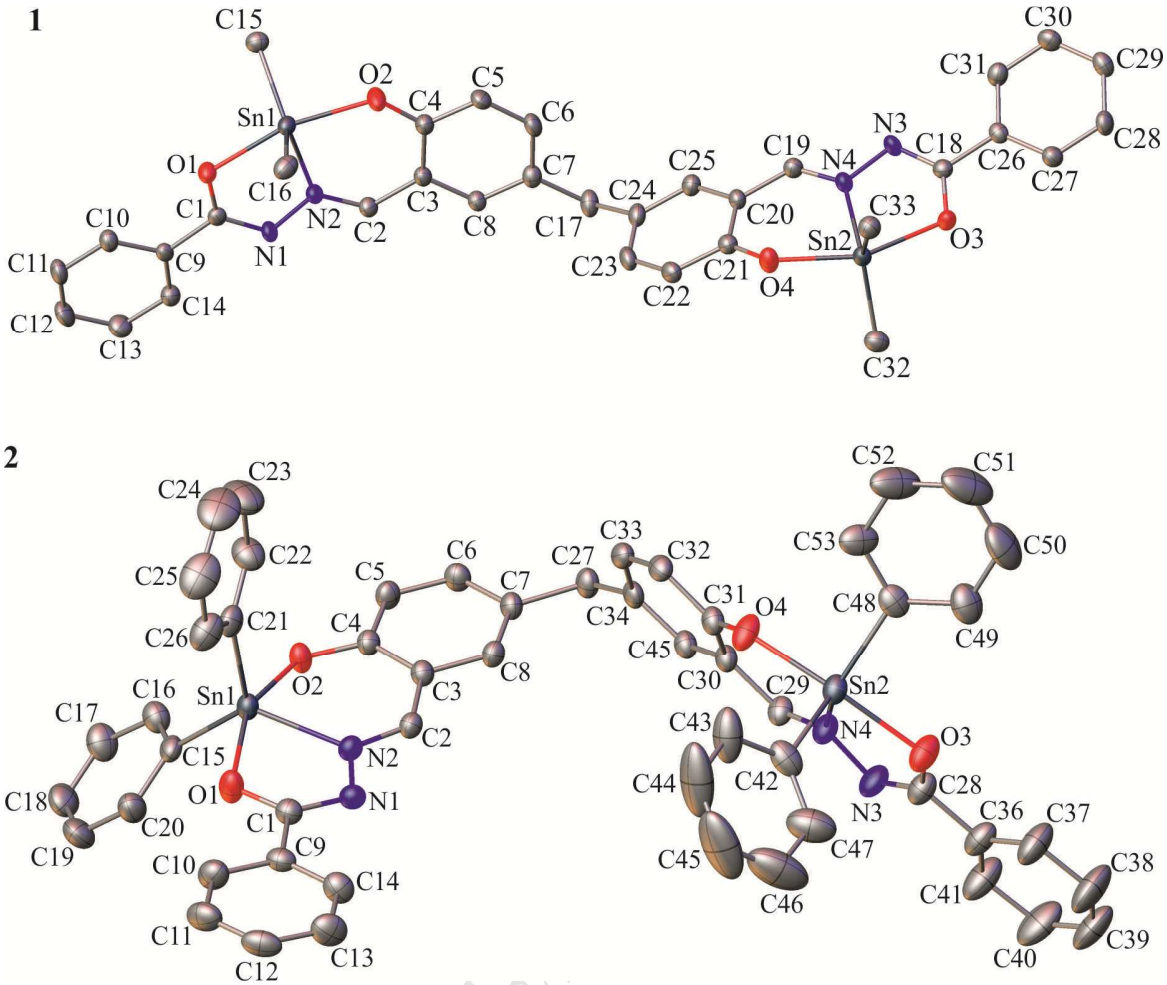

Figure 2. The asymmetric part of the unit cell of **1** and **2** with atom labeling scheme. Displacement ellipsoids were drawn at the 50% probability level. Hydrogen atoms were omitted for clarity.

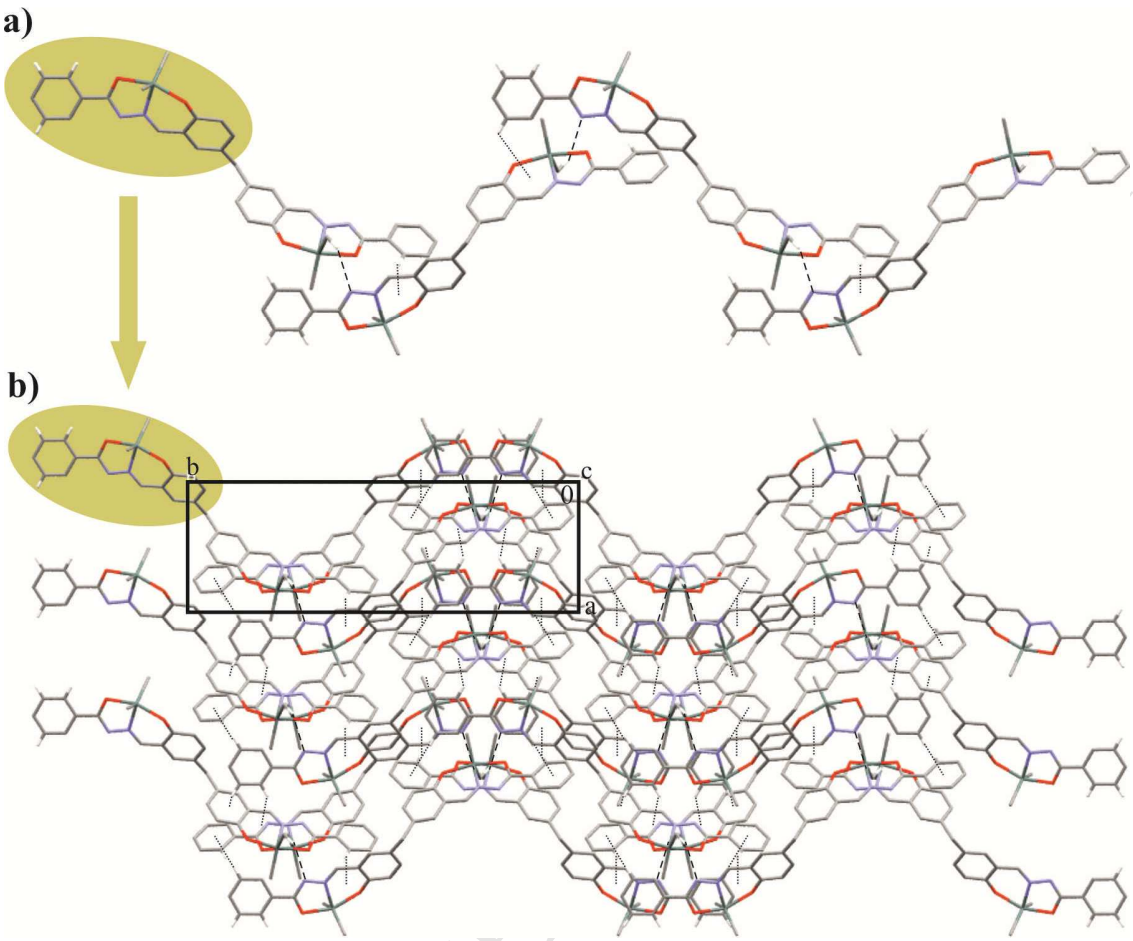

Figure 3 The arrangement of molecules in the crystal of **1**, where: (a) infinite chain of molecules involved in the weak C–H···N hydrogen bonds, running along the b-direction; (b) a general view of the supramolecular framework of molecules along the c-direction. The C–H···N hydrogen bonds are showed as dashed lines, while the weak C–H··π contacts by dotted lines. The H-atoms not participating in the intermolecular interactions were omitted for clarity.

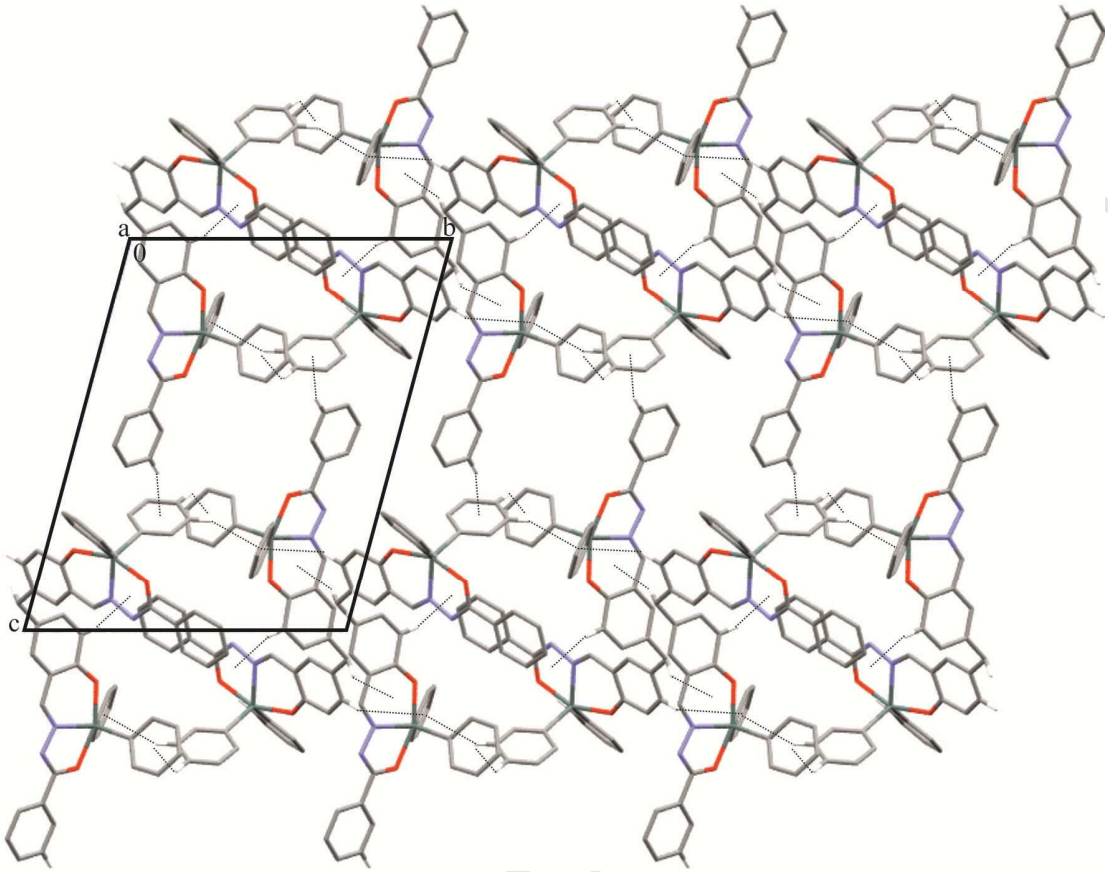

Figure 4. The arrangement of molecules in the crystal of **2** viewed along the a-direction. The weak C–H···π contacts are represented by dotted lines. The H-atoms not participating in the above-mentioned interactions were omitted for clarity.

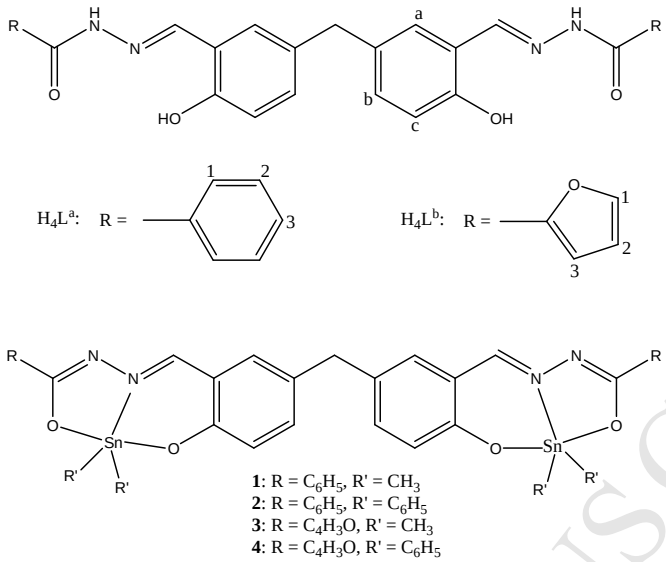

Figure 1 Structure of ligands and complexes with numbering for ^{1}H NMR assignments

Highlight

- Dihydrazones are derived from a methylene-bis-aromatic aldehyde.
- Four dinuclear organotin complexes of dihydrazones were synthesized.
- Dihydrazone is coordinated to two SnR_2 moieties via ONO donor domains.
- Coordination number of both tin is five.
- Antibacterial activity and DNA cleavage of complexes were studied.